

MAGNETIC FIELDS IN NORMAL GALAXIES AND PROSPECTS FOR THE SQUARE KILOMETER ARRAY

R. BECK

Max-Planck-Institut für Radioastronomie
Auf dem Hügel 69
53121 Bonn
Germany
E-mail: rbeck@mpifr-bonn.mpg.de

Grand-design, flocculent and even irregular galaxies host interstellar magnetic fields with a well ordered spiral structure. In grand-design galaxies the fields are aligned parallel to the optical spiral arms, but the strongest regular fields are found in interarm regions, sometimes forming “magnetic spiral arms” between the optical ones. Magnetic fields in the optical spiral arms are strong but irregular, due to tangling by processes related to star formation. Faraday rotation of the polarization vectors shows patterns which support the existence of coherent large-scale fields in galactic disks, signatures of dynamo action. In barred galaxies the magnetic field seems to follow the gas flow within the bar. However, the location of the shock front in the magnetic field deviates from that expected from hydrodynamical models. Within (and interior to) the circumnuclear ring the field is again of spiral shape which leads to magnetic stresses, possibly driving gas inflow towards the active nucleus. The Square Kilometer Array should be able to reveal the wealth of magnetic structures in galaxies.

1 Introduction

Linearly polarized radio continuum emission is a powerful tool to study the strength and structure of interstellar magnetic fields in galaxies. Cosmic-ray electrons spiralling around the field lines emit synchrotron radiation, the dominant contribution to radio continuum emission at centimeter and decimeter wavelengths. If cosmic-ray electrons suffer strong energy losses via synchrotron emission, synchrotron intensity depends mainly on the production rate of cosmic rays [1]. In such a case the synchrotron radio spectrum shows a steepening with decreasing wavelength which, at centimeter wavelengths, is observed only in a few galaxies, e.g. NGC 2276 with its exceptionally strong magnetic field [2]. In a sample of 74 spiral galaxies no tendency of the synchrotron spectral index α to steepen with increasing magnetic field strength was found [3]. The average value is $\alpha = 0.85 \pm 0.02$, with a standard deviation of 0.13 [4]. In conclusion, most galactic spectra are not significantly affected by synchrotron (or inverse Compton) losses, and synchrotron intensity depends on the total field component $B_{t,\perp}$ in the plane of the sky with at least the power $(1 + \alpha)$. The dependence is stronger ($\propto B_{t,\perp}^{3+\alpha}$) if equipartition between cosmic-ray and magnetic field energy densities holds. Equipartition is probably valid on scales of a few kiloparsecs, but may be violated on smaller scales [5] and in strongly interacting galaxies [2].

A map of the total radio intensity (Fig. 1) is a map of the *total interstellar magnetic fields illuminated by cosmic-ray electrons*, polarized intensity (Fig. 2a) reveals the *resolved regular field*. Small-scale variations in radio intensity are mainly due to variations in field strength. The visibility of fields is limited by the diffusion length of cosmic-ray electrons of a few kiloparsecs from their birthplaces in star-forming regions. Thus magnetic fields may still be strong far away from radio-bright regions. Using Faraday rotation measures of background sources, regular fields can be detected until large distances from a galaxy’s center if a halo of ionized gas exists. In M31, for example, the regular field is strong until at least 25 kpc radius [6].

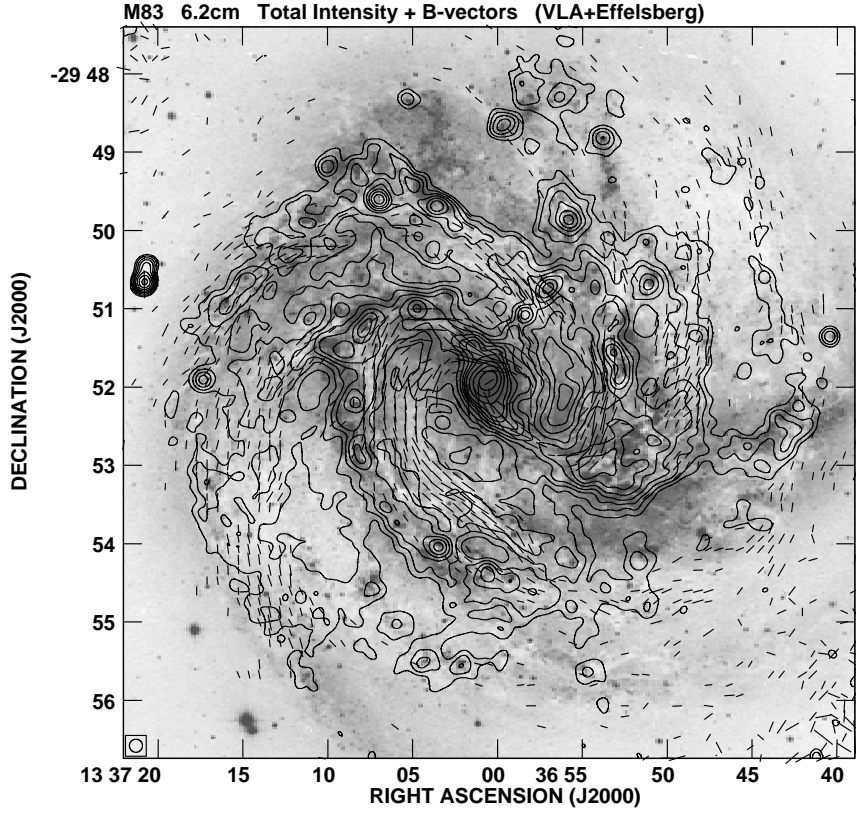


Figure 1: Total radio emission of M83 and B -vectors of polarized emission at $\lambda 6.2$ cm (VLA, $10''$ synthesized beam), combined with the extended emission observed with the Effelsberg 100-m telescope ($2''.5$ resolution) and superimposed onto an optical image of D. Malin (AAO). The length of B -vectors is proportional to polarized intensity. Faraday rotation has not been corrected as it is below 10° (Beck, Ehle, Sukumar & Allen, in prep.)

2 Depolarization and Faraday rotation

Synchrotron emission is highly linearly polarized, intrinsically 70–75% in a completely regular magnetic field. The observable degree of polarization in galaxies is reduced by Faraday (wavelength-dependent) depolarization in magnetized plasma clouds, by geometrical (wavelength-independent) depolarization due to variations of the magnetic field orientation across the telescope beam and along the line of sight, and by a contribution of unpolarized thermal emission (on average 10–20% at centimeter wavelengths, up to 50% locally). Typical fractional polarizations in galaxies are less than a few percent in central regions and spiral arms, 20–40% in between the spiral arms and in outer regions. Thus, polarized radio intensities are weak, and only the largest telescopes are sufficiently sensitive to detect them. The Effelsberg 100-m single-dish telescope provides an angular resolution of $1''.2$ at $\lambda 2.8$ cm and $2''.5$ at $\lambda 6$ cm (Fig. 5). Synthesis telescopes (VLA, ATCA, WSRT) offer higher angular resolution but miss large-scale structures in extended objects like nearby galaxies. Missing flux density in Stokes Q and U maps leads to wrong polarization angles. Combination of single-dish and synthesis data in all Stokes parameters is required (Figs. 1, 2a and 4).

The B -vectors of linearly polarized emission just indicate *anisotropy* of the magnetic field distribution in the emission region. Imagine that a magnetic field without any regular structure (an isotropic random field) is compressed in one dimension by a shock. Emission from the resulting anisotropic field is linearly polarized with ordered B -vectors, but the field is *incoherent*, i.e. it reverses its direction frequently within the telescope beam. *Faraday rotation measures (RM)* are essential to distinguish between coherent and incoherent fields. The sign of RM gives the direction of the field component along the line of sight.

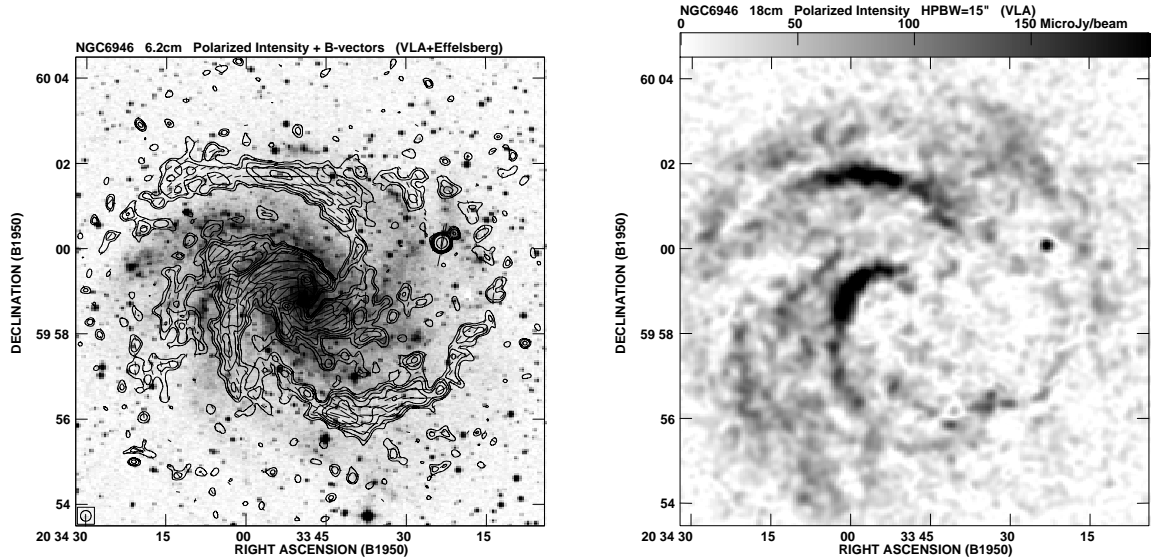


Figure 2: **2a (left)** Polarized radio emission of NGC 6946 at $\lambda 6.2$ cm (VLA, $15''$ synthesized beam), combined with the extended emission observed with the Effelsberg 100-m telescope ($2.5'$ resolution) and superimposed onto an optical image from the POSS. The length of B -vectors is proportional to polarized intensity (from [12])
2b (right) Polarized radio emission of NGC 6946 at $\lambda 18.0$ cm (VLA, $15''$ synthesized beam). Comparison with Fig. 2a reveals regions of Faraday depolarization, especially in the southern and western parts of the galaxy (Beck, in prep.)

At centimeter wavelengths Faraday rotation angles of the polarization vectors vary with λ^2 . Typical interstellar rotation measures of $\simeq 50 \text{ rad/m}^2$ lead to 10° rotation at $\lambda 6 \text{ cm}$ and 3° at $\lambda 3 \text{ cm}$. Below about $\lambda 3 \text{ cm}$ Faraday rotation is so small that the B -vectors (ie. the observed E -vectors rotated by 90°) directly trace the *orientation* of the regular field in the sky plane. To detect small rotation measures, observations at the largest possible wavelength in the Faraday-thin regime are required, e.g. $\lambda \approx 13 \text{ cm}$. Such systems are available at the Effelsberg, ATCA and WSRT telescopes, but not yet at the VLA.

At decimeter wavelengths Faraday depolarization significantly affects the polarized radio emission [7, 8]. Differential Faraday rotation along the line of sight leads to zero polarized intensity (“Faraday shadows”) at certain wavelengths where the observed rotation of the polarization angle reaches multiples of 90° . Hence, filaments of vanishing polarized intensity, accompanied by 90° jumps in polarization angle across the filament, do *not* indicate regions with vanishing electron density or vanishing field strength.

Polarization surveys in our Galaxy have revealed various features in the foreground Faraday screen [9–11]. This opens a new window to study the small-scale field structures. However, true features have to be distinguished from Faraday shadows by mapping in several nearby frequency channels. For example, some small features with zero polarized intensity in NGC 6946 at $\lambda 18 \text{ cm}$ (Fig. 2b) disappear at $\lambda 20 \text{ cm}$ and hence are only “shadows”.

Random fields cause “Faraday dispersion”, and only polarized emission from an upper part of the disk or the halo is detected. Large regions of a galaxy can be depolarized completely (Fig. 2b). Here Faraday rotation angles do no longer vary linearly with λ^2 and RM is no longer proportional to the regular field strength. The observed RM may even change its sign without a reversal in field direction [7].

Nevertheless, polarization data at long wavelengths contain valuable informations: Observations at several nearby wavelengths trace different layers of the galaxy and thus allow *galactic tomography*. (Note, however, that the thickness of the observable layer increases with frequency.)

3 Magnetic field strengths

The average strength of the total $\langle B_{t,\perp} \rangle$ and the resolved regular field $\langle B_{r,\perp} \rangle$ components *in the plane of the sky* can be derived from the total and polarized radio synchrotron intensity, respectively, if energy-density equipartition between cosmic rays and magnetic fields or minimum total energy density is assumed. The standard minimum-energy formulae generally use a fixed integration interval in radio frequency to determine the total energy density of cosmic-ray electrons. This procedure makes it difficult to compare minimum-energy field strengths between galaxies because a fixed frequency interval corresponds to different electron energy intervals, depending on the field strength itself. When instead a fixed integration interval in *energy* is used, the minimum-energy and energy equipartition estimates give similar values for $\langle B_{t,\perp}^{3+\alpha} \rangle$, where α is the synchrotron spectral index (typically $\simeq 0.9$).

The resulting estimate of $\langle B_{t,\perp}^{3+\alpha} \rangle^{1/(3+\alpha)}$ is larger than the mean field $\langle B_{t,\perp} \rangle$ if the field strength varies along the path length. If, on the other hand, the field has a volume filling factor f of smaller than 1, the equipartition estimate is smaller than the field strength in the filaments by a factor $f^{1/(3+\alpha)}$ [13].

Nothing is known about f yet.

The mean magnetic field strength for the sample of 74 spiral galaxies is $\langle B_{t,\perp} \rangle = 9 \mu\text{G}$ (0.9 nT) with a standard deviation of $3 \mu\text{G}$ [14]. In nearby galaxies the average total field strengths in the galactic plane (corrected for inclination) range between $\langle B_t \rangle \simeq 4 \mu\text{G}$ in M33 [15] and $\simeq 15 \mu\text{G}$ in M51 [16]. In spiral arms the total field strengths can reach $\simeq 20 \mu\text{G}$ locally, like in NGC 6946 [17], M51 and M83.

Interacting galaxies host even stronger magnetic fields, probably larger than the equipartition values [2]. The strongest field within a normal galaxy found so far is that in the circumnuclear ring of NGC 1097 with $B_t \simeq 40 \mu\text{G}$ [18]. The strengths of the resolved regular fields B_r are typically 1–5 μG locally, but $\simeq 13 \mu\text{G}$ in an interarm region of NGC 6946 (Sect. 6); these are always lower limits due to the limited angular resolution.

4 Magnetic fields and gas clouds

Comparison of the maps of the total radio emission of M51 [19] and the total (cold + warm) dust emission [20] reveals a surprisingly close connection. To understand its origin it is crucial to consider the strong (probably dominant) influence of the field strength on radio intensity. Magnetic fields are obviously anchored in gas clouds which are traced by the dust. Remarkably, one dust lane crosses the eastern spiral arm of M51, and so does the total field. Furthermore, the total radio and far infrared luminosities of galaxies are tightly correlated. The correlation can be explained, globally and locally and with the correct slope, by a close coupling of magnetic fields to gas clouds [3, 5]. The radio – far-infrared correlation within M31 indicates that the coupling is valid even for the more diffuse gas mixed with cool dust [5]. The detailed comparison between the total synchrotron intensity and the cool gas ($\text{HI} + 2\text{H}_2$) in a spiral arm of M31 confirmed a coupling of the magnetic field to the gas [21]. The total field strength B_t is high in spiral arms because the gas density is highest there.

The correlation between gas and *regular* fields is less obvious. Long, prominent dust lanes are often connected to features of regular fields, e.g. in M83 (Fig. 1), in the anomalous arm of NGC 3627 [22] and in flocculent galaxies like NGC 4414 (Fig. 3). On the other hand, regular fields are sometimes observed in interarm regions with very little gas or dust (Sect. 6).

5 Magnetic field structure

Grand-design spiral galaxies are shaped by density waves, but the role of magnetic fields is yet unknown. Strong shocks should compress the magnetic field and increase the degree of radio polarization on the inner edges of the spiral arms. Radio observations, however, show a larger variety of phenomenae.

The total radio intensity shows the total (=regular+random) field, the polarized radio intensity the resolved regular field only. The strongest total and regular fields in M51 are found at the positions of the prominent dust lanes on the inner edges of the optical spiral arms [19], as expected from compression

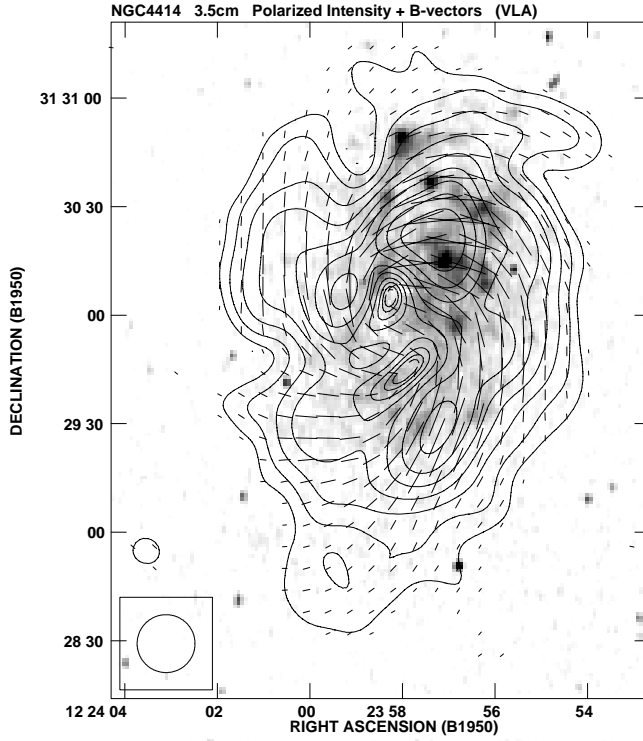


Figure 3: Polarized radio emission of the flocculent galaxy NGC 4414 at $\lambda 3.5$ cm (VLA, $16''$ synthesized beam), superimposed onto an optical H α image obtained by C. Horellou. The length of B -vectors is proportional to polarized intensity (Soida et al., in prep.)

by density waves, but the regular fields extend far into the interarm regions. In M83 (Fig. 1) the total and polarized emission peak on the inner edge of the northern optical arm; in the southern arm the total emission shows no shift with respect to the optical arm, while the polarized emission is strongly shifted into the interarm region between the southern arm and the bar. NGC 1566 [23] and M81 [24] show almost no signs of field compression; their strongest regular fields occur in *interarm regions*, while the total field is still highest in the optical spiral arms. Field tangling in the spiral arms, e.g. due to increased turbulent motions of gas clouds and supernova shock fronts, may explain this result [25]. In some cases, however, the interarm fields are concentrated in “magnetic arms” which cannot be explained by the lack of field tangling (see Sect. 6).

Radio polarization observations show that the B -vectors of the regular fields largely follow the optical spiral structure in M51 [16, 19], M81 [24], M83 (Fig. 1) and NGC 1566 [23], though generally *offset* from the optical arms. In the density-wave picture the magnetic field is frozen into the gas clouds and is transported by the gas flow. Thus the field orientation should reflect the streaming lines of the gas, not the structure of the spiral wave itself. The pitch angles of the streaming lines are small in interarm regions and larger in spiral arms (though still smaller than that of the spiral wave). However, the observed pitch angles of the regular field are larger than those of the streaming lines almost everywhere. In the interarm regions of NGC 6946 the field pitch angle is $\simeq 20^\circ$ [26], while the gas flow is almost azimuthal. Hence, the regular magnetic field is not frozen into the gas flow, but probably modified by turbulent diffusion [27] and/or shaped by dynamo action (Sect. 7).

Regular spiral magnetic fields with strengths similar to those in grand-design galaxies have been detected in flocculent galaxies (Fig. 3) and even in irregular galaxies (Fig. 4). The mean degree of polarization (corrected for different spatial resolutions) is similar between grand-design and flocculent galaxies [28]. Apparently, density waves have a relatively small effect on the field structure.

In our Galaxy several field reversals between the spiral arms, on kpc scales, have been detected from pulsar rotation measures [29, 30]. Polarization observations of some external galaxies have sufficiently

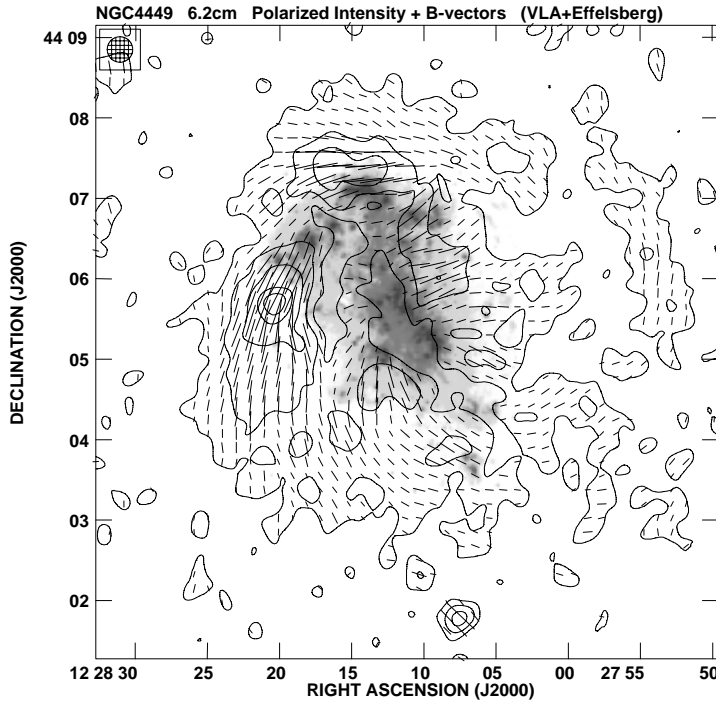


Figure 4: Polarized radio emission of the irregular galaxy NGC 4449 at $\lambda 6.2$ cm (VLA, $19''$ synthesized beam), combined with the extended emission observed with the Effelsberg 100-m telescope ($2.5'$ resolution), and superimposed onto an optical H α image obtained by D. Bomans. The length of B -vectors is proportional to polarized intensity (from [31])

high spatial resolution, but similar reversals have not yet been detected in the maps of rotation measures, e.g. within the main emission “ring” of M31 (Fig. 5). For other galaxies like M51, M83 and NGC 6946 the evidence against reversals is weaker but still significant. Field reversals may occur preferably in galaxies with less organized spiral structure. Another explanation is that pulsar RMs in the Galaxy trace the field near the Galactic plane while RMs in external galaxies show the average regular field along the pathlength through the “thick disk” (see Sect. 8).

There is increasing observational evidence that magnetic fields are important for the formation of spiral arms. The streaming velocity and direction of gas clouds and their collision rates can be modified. Furthermore, magnetic fields will also influence the star formation rates in spiral arms. Magnetic fields are essential for the onset of star formation as they allow to remove angular momentum from the protostellar cloud during its collapse.

6 Magnetic spiral arms

Long arms of polarized emission were discovered in IC 342 [32, 33]. Observations of another gas-rich galaxy, NGC 6946 [12], revealed a surprisingly regular distribution of polarized intensity with two “magnetic arms” located in *interarm* regions, without any association with cool gas or stars, running parallel to the adjacent optical spiral arms (Fig. 2a). These magnetic arms do not fill the entire interarm spaces like the polarized emission in M81, but are only $\simeq 500\text{--}1000$ pc wide. The fields in the magnetic arms must be *almost totally aligned*, and the peak strength of the regular field is $\simeq 13 \mu\text{G}$. Magnetic arms have also been found in M83 (Fig. 1, south of the bar) and in NGC 2997 [34].

The magnetic arms cannot be artifacts of depolarization. Firstly, their degree of polarization is exceptionally high (up to 50%). Secondly, they look quite similar at $\lambda 6$ cm and $\lambda 3$ cm. Thirdly, they are also visible as peaks in total emission, which excludes their existence solely due to a window in geometrical depolarization (small field tangling).

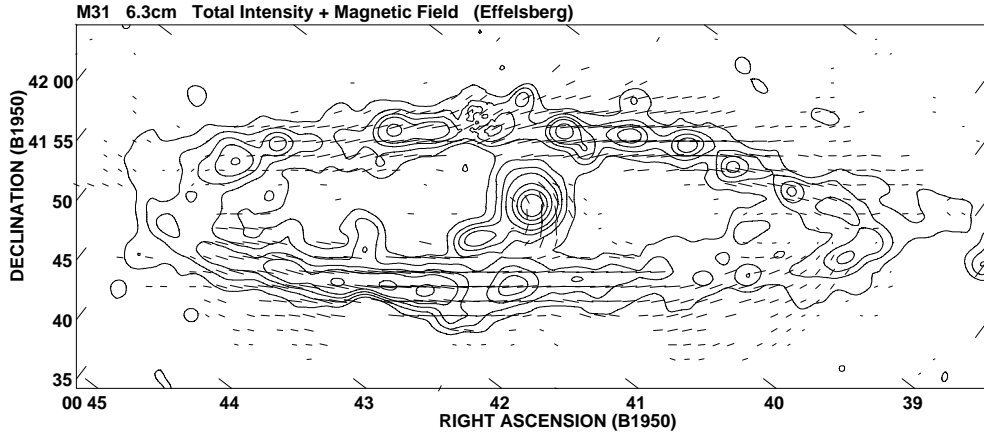


Figure 5: Total intensity of M31 at $\lambda 6.3$ cm (Effelsberg 100-m telescope, smoothed to $3'$ resolution), and magnetic field orientations at $5'$ resolution. Faraday rotation has been corrected with help of Effelsberg data at $\lambda 11.1$ cm with $5'$ resolution. The length of vectors is proportional to polarized intensity (Berkhuijsen, Beck & Hoernes, in prep.)

We still do not understand how magnetic arms are generated. It was proposed that they could be manifestations of slow MHD waves which may propagate in a rigidly rotating disk, with the maxima in field strength phase-shifted against those in gas density [35]. However, all galaxies with magnetic arms rotate differentially beyond 1–2 kpc from the centre. Some correlation exists between the magnetic arms and interarm gas features generated in numerical models of perturbed galactic disks [36]. However, such models neglect the effect of magnetic fields. In dynamo models, using the reasonable assumption that the dynamo number is larger between the optical arms than in the arms [37], magnetic arms evolve between the optical arms in a differentially rotating disk [26, 38, 39]. However, the back-reaction of the field onto the gas has not been considered yet in present-day dynamo models. In the magnetic arms the energy density of the field may exceed that of the large-scale gas motion and thus distort the gas flow.

7 Faraday rotation and dynamos

Regular magnetic fields could in principle be shaped by gas flows and density waves. Faraday rotation measures (RM) are essential to distinguish between coherent and incoherent fields. In an incoherent field the RM s are random and show no large-scale structure. Observation of RM *coherency* on a large scale, like in M31 [6, 40], NGC 6946 [41] and NGC 2997 [34], means that the field was coherent already before compression, and hence there must be another physical mechanism (dynamo or primordial origin) to generate such an ordered field. The role of density waves would then be restricted to the alignment of the large-scale coherent field with the spiral arms.

The strongest evidence for dynamo action comes from M31 (Fig. 5). Radio observations of M31 revealed a 20 kpc-sized torus of magnetic fields aligned in *a single direction* [40]. Only the dynamo is able to generate a unidirectional field of such dimensions. RM s from polarized background sources confirmed this picture [6]. The regular field exists also interior to the prominent “ring” and extends out to at least 25 kpc radius.

Dynamos are promising candidates to generate coherent fields, even in galaxies without density waves. The linear mean-field dynamo [13, 42] generates magnetic field modes which have spiral structure due to their azimuthal and radial field components. The pitch angle of the field spiral depends on the dynamo number, *not* on the pitch angle of the gas spiral. The field structure is described by modes of different azimuthal and vertical symmetry; in general a superposition of modes is generated. A large-scale pattern in maps of Faraday rotation measures (RM s) reveals the dominance of a single dynamo mode [43]. A single-periodic azimuthal RM variation (with a phase equal to the pitch angle of the spiral structure) indicates a dominating axisymmetric dynamo mode (ASS, $m = 0$), as in

M31 [6, 40] and IC 342 [32]. Double-periodic azimuthal RM variations indicate a dominating bisymmetric dynamo mode (BSS, $m = 1$) if their phases vary with radial distance as expected [43], as is the case for M81 [24] and possibly M33 [15]. The interacting galaxy M51 is a special case. Analyzing all available polarization angle data, the field in M51 can be described as mixed modes (MSS), with axisymmetric and bisymmetric components having about equal weights in the disk, together with a horizontal axisymmetric halo field with opposite direction [44]. The magnetic arms of NGC 6946 may be the result of a superposition of the ASS and the quadrисymmetric ($m = 2$) modes, while the BSS mode is suppressed by the two-armed spiral structure of the gas [26]. In many other galaxies the data are still insufficient to allow a firm conclusion whether the large-scale pattern of the regular field is even more complicated or the distribution of thermal gas is non-axisymmetric so that the RMs are distorted. The similarity of pitch angles between the dynamo-wave and the density-wave spiral is not self-evident and indicates the existence of some interaction between them. Future dynamo models have to include density waves and the back-reaction of the field.

By comparing the signs of the RM distribution and the velocity field, inward and outward directions of the radial component of the spiral magnetic field can be distinguished. Surprisingly, all known ASS fields (M31, IC 342, NGC 253) and the MSS field in NGC 6946 point *inwards*. Dynamo action does not prefer one direction. This indicates some asymmetry in the initial seed field and excludes small-scale seed fields [41], possibly a cosmologically relevant result. A larger data base is needed.

8 Edge-on galaxies and radio halos

NGC 891, NGC 5907 and NGC 7331 and other edge-on galaxies possess *thick radio disks* with $\simeq 1$ kpc scale heights. In these galaxies the observed field orientations are mainly parallel to the disk [45]. NGC 4565 has the most regular plane-parallel field [46]. Bright, extended radio halos (with scale heights of several kpc) are rare. NGC 253 is the edge-on galaxy with the brightest and largest halo observed so far [47]. The irregular appearance of the NGC 253 halo is mainly due to the lower sensitivity compared with the map of NGC 4631. The regular magnetic field in the disk of NGC 253 is also predominantly parallel to the plane [48] which may be due to strong dynamo action even close to the centre. Some radio spurs with vertical field lines emerge from the outer disk.

NGC 4631, NGC 4666 and M82 are halo galaxies with dominating vertical field components [49–52]. Magnetic spurs in these halos are connected to star-forming regions in the disk. The field is probably dragged out by the strong, inhomogenous galactic wind. Evidence was found for a direct dependence of the halo extent on the level of energy input from the underlying disk [53]. The magnetic field lines in the NGC 4631 halo have a dipolar structure (Fig. 6) in the inner disk where differential rotation is weak so that the dipolar (antisymmetric) dynamo mode can evolve. A few regions with field orientations parallel to the disk are visible in the (differentially rotating) outer disk. Maps of rotation measures are required to test the dipolar model.

In the planes of edge-on spiral galaxies the observed polarized emission is weak due to depolarization effects. Faraday depolarization alone is insufficient to explain the low degrees of polarization near the plane of NGC 4631 [50]. The field structure in the plane is mostly turbulent due to star-forming processes, causing depolarization along the line of sight as well as across the telescope beam [45]. The degree of polarization at high frequencies increases with increasing distance from the plane because the star-forming activity and thus the field turbulence decrease.

9 Barred galaxies

Gas and stars in barred galaxies move in highly noncircular orbits. Gas streamlines are strongly deflected in the bar region along shock fronts, behind which the gas is compressed in a fast shearing flow [54]. As the gas in the bar region rotates faster than the bar, compression regions traced by massive dust lanes develop along the edge of the bar that is leading with respect to the galaxy's rotation. Gas inflow along the compression region may fuel starburst activity in a dense ring near the galactic centre, although it is not clear how the gas can get rid of its angular momentum before falling into the active

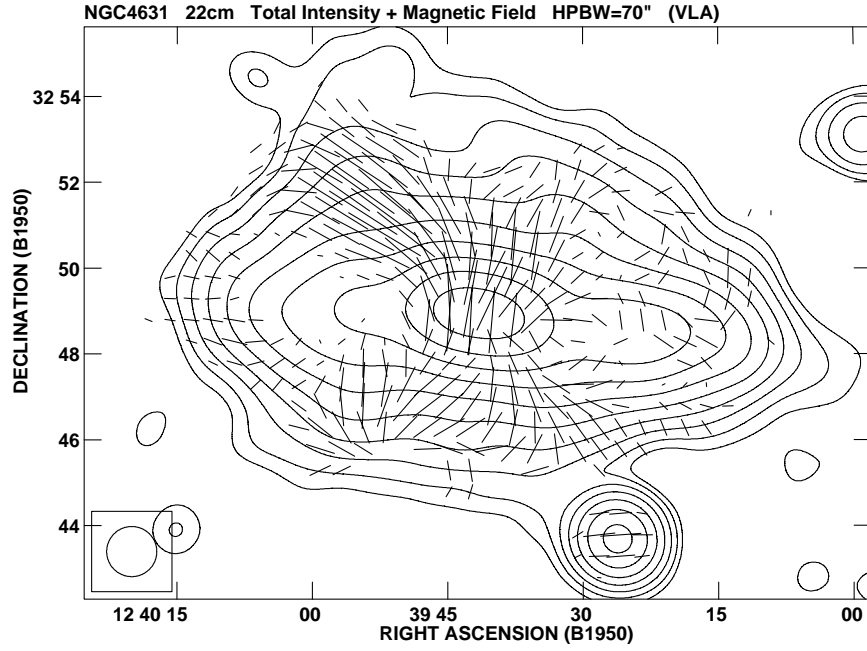


Figure 6: Total radio emission and B -vectors of polarized emission of NGC 4631 at $\lambda 22$ cm (VLA, $70''$ synthesized beam). The B -vectors have been corrected for Faraday rotation, their length is proportional to polarized intensity (Krause et al., in prep.)

nucleus. The effects of magnetic fields on gas flows in barred galaxies have not yet been addressed in models.

From a sample of galaxies with strong optical bars observed with the Effelsberg, VLA and ATCA telescopes, the strongest regular magnetic fields were detected in NGC 1097, NGC 1365, NGC 4535 and NGC 7479. NGC 1097 and NGC 1365 are barred galaxies of morphological type SBbc with their bars lying almost in the plane of the sky so that spectroscopic observations of the shearing gas flow are very difficult.

The general similarity of the B -vectors in NGC 1097 (Fig. 7) and gas streamlines around the bar as obtained in simulations [54] is striking. This suggests that the regular magnetic field is aligned with the shearing flow. We observe ridges of enhanced total magnetic fields which coincide with the optical dust lanes. The upstream and downstream regions of enhanced polarized emission are separated by a strip of zero polarized intensity, the location of the shock front, where the observed B -vectors change their orientation abruptly (Fig. 7). This large deflection angle leads to geometrical depolarization within the telescope beam because the strip where the field changes its direction is narrower than the spatial resolution of our observations. Our polarization observations imply that the shock front in the magnetic field is located 700–900 pc in front of the dust lanes, in contrast to conditions in classical shocks.

Furthermore, the degree of field alignment is largest upstream (with a degree of polarization of up to 50%, right half of the bar in Fig. 7), not downstream. This indicates that the shock generates field turbulence. Numerical models including magnetic fields are required. Strong deflections of the B -vectors are also observed in the bar of M83 (Fig. 1) and in NGC 1672 (Fig. 8).

The circumnuclear ring of NGC 1097 is a site of ongoing intense star formation, with an active nucleus in its centre. The local equipartition strengths of the total and regular magnetic fields are $B_t \simeq 40\mu\text{G}$ and $B_r \simeq 7\mu\text{G}$ in the ring. The field strength reaches its absolute maximum where the compression region intersects with the ring. The regular field swings from alignment along the bar to a spiral pattern near the ring [18]. In contrast to the bar, conditions for dynamo action are ideal in the ring. The orientation of the innermost field agrees with that of the spiral dust filaments visible in the optical HST image. Magnetic stress in the circumnuclear ring can drive mass inflow to feed the active nucleus in NGC 1097.

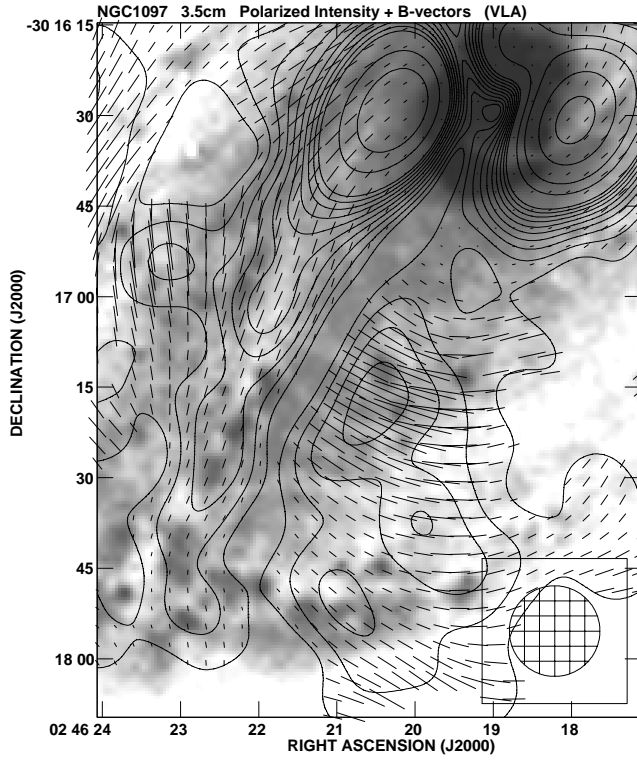


Figure 7: Total emission and B -vectors of polarized radio emission of the southern half of the barred galaxy NGC 1097 at $\lambda 3.5$ cm (VLA, $15''$ synthesized beam), superimposed onto an optical image of H. Arp (MPE/Cerro Tololo). The length of B -vectors is proportional to *the degree of polarization*. (from [18])

Our results have revealed a principal difference between the behaviours of magnetic fields in barred and non-barred galaxies. In bars the magnetic field appears to interact strongly with the gas flow. In non-barred galaxies the field lines are of overall spiral shape so that the regular fields do *not* follow the gas flow, which is typical for dynamo-generated fields.

10 Open questions

All gas-rich galaxies, even irregular ones, host fields of $\simeq 1$ nT strength. If the fields do not fill the whole interstellar space, they are even stronger. The dynamical importance of magnetic fields in galaxies cannot be neglected anymore. Increasing resolution of the radio telescopes and higher sensitivity of the receiver systems revealed a spectrum of features: On largest scales, extended spiral fields of different symmetry modes were found, typical signatures of dynamo action. How the field can adopt a similar pitch angle as that of the optical spiral remains a mystery. The preferred *inward* direction of axisymmetric fields, if confirmed by future observations, also awaits explanation. On intermediate scales, “magnetic arms” between the optical spiral arms (Figs. 1,2a) are still puzzling as they seem to be disconnected from the gas. On the other hand, fields can also be aligned by gas flows in density-wave and bar potentials. The unexpected location of the shock front in a barred galaxy (Fig. 7) tells us that strong magnetic fields interact with the gas flow, but details are still unobservable. Radio halos are the result of magnetic fields pulled outwards by galactic winds. Alternatively, dynamo-generated dipolar fields (Fig. 6) may enhance the wind. Some structures in radio halos show similarities to those in the solar corona: loops, spurs [50] and possibly coronal holes [17].

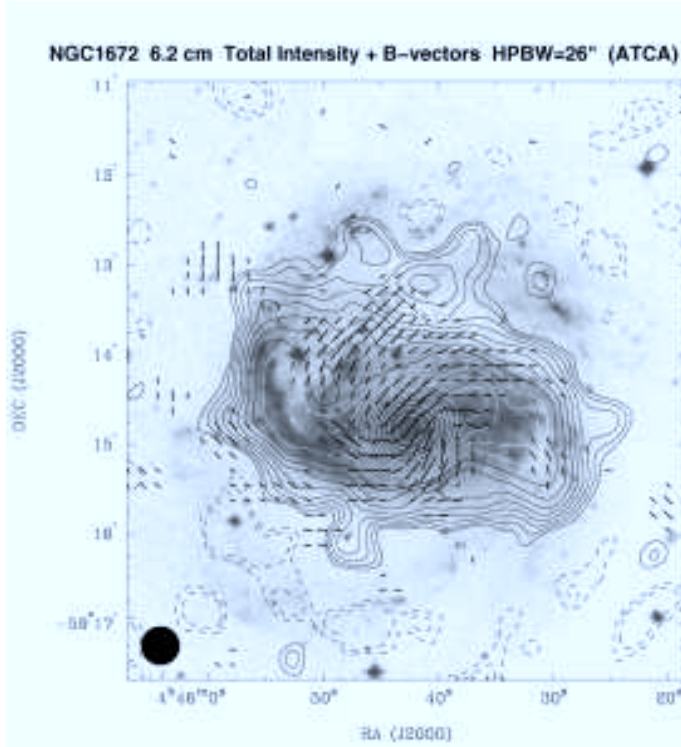


Figure 8: Total emission and B -vectors of polarized radio emission of the barred galaxy NGC 1672 at λ 6.2 cm (ATCA, $26''$ synthesized beam), superimposed onto a Digital Sky Survey (DSS) optical image. The length of B -vectors is proportional to the polarized intensity (Ehle, Haynes, Beck et al., unpublished)

11 Limitations of present-day polarization observations

Regular fields in galaxies show structures on kiloparsec scales which can be observed with present-day radio telescopes. Typical polarized intensities at λ 6 cm are $50\text{--}100\mu\text{Jy}$ per $15''$ beam (VLA D configuration, smoothed). In case of equipartition between cosmic-ray and magnetic field energy densities and assuming a constant field strength along a pathlength of 1 kpc, these intensities correspond to regular fields of $5\text{--}6\mu\text{G}$ strength. The $15''$ beam can resolve only 730 pc at 10 Mpc distance, thus the detailed field structure remains unexplored. With the next higher VLA configuration ($\simeq 5''$ beam) the polarized intensity drops to $5\text{--}10\mu\text{Jy}$ per beam which cannot be detected within reasonable time. For example, only the circumnuclear ring of NGC 1097 is visible in polarized emission at λ 6 cm and λ 3 cm with the VLA C-configuration. Within the optical spiral arms polarized emission is even lower due to field tangling on scales of 10–100 pc. Hence, while the VLA in principle provides sufficiently high angular resolution, *its sensitivity is too low to study the detailed field structure*.

Another limitation is galactic distance. Though radio intensity per unit beamsize is distance-independent, more distant galaxies can be observed with the same signal-to-noise ratio only as long as the spatial resolution is sufficient to resolve them. If the large-scale structure of the magnetic field is not fully resolved, polarized intensity decreases due to geometrical depolarization across the beam. The curvature of a spiral field is significant beyond a scale of $\simeq 5$ kpc, thus we lose polarized intensity per standard $15''$ beam for galaxies beyond $\simeq 70$ Mpc distance. Again, using the next larger VLA configuration does not help because the intensity drops by a factor of $\simeq 10$. Hence, polarization observations of distant galaxies are *sensitivity-limited*, too.

With the Square Kilometer Array the field structures could be observed of 10x more distant galaxies which are several Gyr younger than the nearby objects. The dynamo timescale is some 10^9 yr [13] so that weaker or less regular fields may be expected at larger distances. Using Faraday rotation mapping, even younger galaxies can be observed (see below).

Faraday rotation measures of background sources can trace magnetic fields to larger radii than polarized intensity. Within the disks, the ratio between internal RM and background RM allows to detect field reversals along the line of sight. However, the number of available sources is very low. In the M31 field (≈ 1.5 square degrees) only 22 background sources with polarized flux densities higher than 0.3 mJy were found at $\lambda 20$ cm within 1 hour VLA on-source observation time [6]. In a much smaller field like that of NGC 6946, the number of available sources drops to less than 1. Even within several hours observation time only a few polarized background sources are detectable. The much better sensitivity of the SKA will allow for the first time a systematic RM mapping of galaxies.

Signatures of a regular field with a bisymmetric spiral structure were detected in the intervening ($z = 0.395$) galaxy in front of PKS 1229–021 [55]. The SKA will allow such studies of the magnetic field structure in very young galaxies with higher resolution and much better sensitivity.

12 Prospects for the Square Kilometer Array

- High-resolution polarization mapping at centimeter wavelengths:
 - Polarized intensities at different spatial resolutions to obtain the turbulence spectrum of the regular field, to be compared with models of field generation and destruction
 - Detailed comparison between magnetic fields and gas components of various temperatures and densities: Which gas components interact with the field?
 - Detailed comparison between fields and the gas flow in star-forming regions, spiral arms, bars, central rings: What tangles the field? Where is the field frozen into the gas flow, where does it diffuse away?
 - Field structure in halos: Search for loops, streamers, coronal holes and indications for magnetic reconnection
 - Needed: Systems in the Faraday-thin regime (≥ 5 GHz)
- High-resolution polarization mapping at decimeter wavelengths:
 - Field structure in the foreground Faraday screen
 - ISM tomography
 - Needed: Systems with a large number of bands (0.3–2 GHz)
- High-resolution Faraday mapping:
 - Direction of axisymmetric spiral fields
 - Search for field reversals in disks
 - Reversals in halos: Wind or dynamo?
 - Polarized background sources: Extent of nearby magnetic disks
 - Distant polarized radio galaxies: Field structure in intervening galaxies
 - Needed: Systems between 2 GHz and 10 GHz
- High-resolution Zeeman mapping (beyond the scope of this paper)

References

- [1] H.J. Völk, *Astronomy & Astrophysics* 218, 67–70 (1989)
- [2] E. Hummel, R. Beck, *Astronomy & Astrophysics* 303, 691–704 (1995)
- [3] S. Niklas, R. Beck, *Astronomy & Astrophysics* 320, 54–64 (1997)
- [4] S. Niklas, U. Klein, R. Wielebinski, *Astronomy & Astrophysics* 322, 19–28 (1997)
- [5] P. Hoernes, E.M. Berkhuijsen, C. Xu, *Astronomy & Astrophysics* 334, 57–70 (1998)

- [6] J.L. Han, R. Beck, E.M. Berkhuijsen, *Astronomy & Astrophysics* 335, 1117-1123 (1998)
- [7] D.D. Sokoloff, A.A. Bykov, A. Shukurov, E.M. Berkhuijsen, R. Beck, A.D. Poezd, *Monthly Notices of the Royal Astronomical Society* 299, 189-206 (1998) and 303, 207-208 (1999) (Erratum)
- [8] M. Urbanik, D. Elstner, R. Beck, *Astronomy & Astrophysics* 326, 465-476 (1997)
- [9] M.H. Wieringa, A.G. de Bruyn, D. Jansen, W.N. Brouw, Katgert P., *Astronomy & Astrophysics* 268, 215-229 (1993)
- [10] A.D. Gray, T.L. Landecker, P.E. Dewdney, A.R. Taylor, *Nature* 393, 660-662 (1998)
- [11] B. Uyaniker, E. Fürst, W. Reich, P. Reich, R. Wielebinski, *Astronomy & Astrophysics Suppl. Ser.* 138, 31-45 (1999)
- [12] R. Beck, P. Hoernes, *Nature* 379, 47-49 (1996)
- [13] R. Beck, A. Brandenburg, D. Moss, A. Shukurov, D. Sokoloff, *Annual Reviews Astronomy & Astrophysics* 34, 155-206 (1996)
- [14] S. Niklas, PhD Thesis, University of Bonn (1995)
- [15] U.R. Buczilowski, R. Beck, *Astronomy & Astrophysics* 241, 47-56 (1991)
- [16] N. Neininger, *Astronomy & Astrophysics* 263, 30-36 (1992)
- [17] R. Beck, *Astronomy & Astrophysics* 251, 15-26 (1991)
- [18] R. Beck, M. Ehle, V. Shoutenkov, A. Shukurov, D. Sokoloff, *Nature* 397, 324-327 (1999)
- [19] N. Neininger, C. Horellou, 1996, in *Polarimetry of the Interstellar Medium* (Astr. Soc. Pacific), Edited by W.G. Roberge & D.C.B. Whittet, p. 592-597
- [20] D.L. Block, B.G. Elmegreen, A. Stockton, M. Sauvage, *The Astrophysical Journal* 486, L95-98 (1997)
- [21] E.M. Berkhuijsen, E. Bajaja, R. Beck, *Astronomy & Astrophysics* 279, 359-375 (1993)
- [22] M. Soida, M. Urbanik, R. Beck, R. Wielebinski, *Astronomy & Astrophysics* 345, 461-470 (1999)
- [23] M. Ehle, R. Beck, R.F. Haynes, A. Vogler, W. Pietsch, M. Elmouttie, S. Ryder, *Astronomy & Astrophysics* 306, 73-85 (1996)
- [24] M. Krause, R. Beck, E. Hummel, *Astronomy & Astrophysics* 217, 17-30 (1989)
- [25] S. Sukumar, R.J. Allen, *Nature* 340, 537-539 (1989)
- [26] R. Rohde, R. Beck, D. Elstner, *Astronomy & Astrophysics* (1999), in press
- [27] S. von Linden, K. Otmianowska-Mazur, H. Lesch, G. Skupniewicz, *Astronomy & Astrophysics* 333, 79-91 (1998)
- [28] J. Knapik, M. Soida, R.-J. Dettmar, R. Beck, M. Urbanik, *Astronomy & Astrophysics* (1999), in press
- [29] A.G. Lyne, F.G. Smith, *Monthly Notices of the Royal Astronomical Society* 237, 533-541 (1989)
- [30] J.L. Han, R.N. Manchester, G.J. Qiao, *Monthly Notices of the Royal Astronomical Society* 306, 371-380 (1999)
- [31] K.T. Chyzy, R. Beck, S. Kohle, U. Klein, M. Urbanik M., *Astronomy & Astrophysics* (1999), submitted
- [32] M. Krause, E. Hummel, R. Beck, *Astronomy & Astrophysics* 217, 4-16 (1989)
- [33] M. Krause, 1993, in *The Cosmic Dynamo* (Kluwer, Dordrecht), Edited by F. Krause et al., p. 305-310
- [34] J.L. Han, R. Beck, M. Ehle, R.F. Haynes, R. Wielebinski, *Astronomy & Astrophysics* 348, 405-417 (1999)
- [35] Z. Fan, Y.-Q. Lou, *Monthly Notices of the Royal Astronomical Society* 291, 91-109 (1997)
- [36] P.A. Patsis, P. Grosbol, N. Hiotelis, *Astronomy & Astrophysics* 323, 762-774 (1997)
- [37] A. Shukurov, *Monthly Notices of the Royal Astronomical Society* 299, L21-24 (1998)
- [38] D. Moss, *Monthly Notices of the Royal Astronomical Society* 297, 860-866 (1998)
- [39] R. Rohde, D. Elstner, *Astronomy & Astrophysics* 333, 27-30 (1998)
- [40] R. Beck, *Astronomy & Astrophysics* 106, 121-132 (1982)
- [41] F. Krause, R. Beck, *Astronomy & Astrophysics* 335, 789-796 (1998)
- [42] R. Wielebinski, F. Krause, *The Astronomy & Astrophysics Reviews* 4, 449-485 (1993)
- [43] M. Krause, 1990, in *Galactic and Intergalactic Magnetic Fields* (Kluwer, Dordrecht), Edited by R. Beck et al., p. 187-196

- [44] E.M. Berkhuijsen, C. Horellou, M. Krause, N. Neininger, A. Poezd, A. Shukurov, D. Sokoloff, *Astronomy & Astrophysics* 318, 700-720 (1997)
- [45] M. Dumke, M. Krause, R. Wielebinski, U. Klein, *Astronomy & Astrophysics* 302, 691-703 (1995)
- [46] S. Sukumar, R.J. Allen, *The Astrophysical Journal* 382, 100-107 (1991)
- [47] C.L. Carilli, M.A. Holdaway, P.T.P. Ho, C.G. de Pree, *The Astrophysical Journal* 399, L59-62 (1992)
- [48] R. Beck, C.L. Carilli, M.A. Holdaway, U. Klein, *Astronomy & Astrophysics* 292, 409-424 (1994)
- [49] E. Hummel, R. Beck, M. Dahlem, *Astronomy & Astrophysics* 248, 23-29 (1991)
- [50] G. Golla, E. Hummel, *Astronomy & Astrophysics* 284, 777-792 (1994)
- [51] M. Dahlem, M.G. Petr, M.D. Lehnert, T.M. Heckman, M. Ehle, *Astronomy & Astrophysics* 320, 731-745 (1997)
- [52] H.-P. Reuter, U. Klein, H. Lesch, R. Wielebinski, P.P. Kronberg, *Astronomy & Astrophysics* 282, 724-730 (1994)
- [53] M. Dahlem, U. Lisenfeld, G. Golla, *The Astrophysical Journal* 444, 119-128 (1995)
- [54] E. Athanassoula, *Monthly Notices of the Royal Astronomical Society* 259, 345-364 (1992)
- [55] P.P. Kronberg, J.J. Perry, E.L.H. Zukowski, *The Astrophysical Journal* 387, 528-535 (1992)